ACS OMEGA

Open Access

http://pubs.acs.org/journal/acsodf

Article

Folic Acid–Intercalated Mg/Al Layered Double Hydroxides—A Multifunctional Nanohybrid Delivery System for Topical Applications

Phumelele Kleyi, Vusani Mandiwana, Marinda de Beer, Sreejarani Kesavan Pillai, and Suprakas Sinha Ray*

Cite This: *ACS Omega* 2024, 9, 48185−48195

Read Online

ACCESS | Metrics & More | Article Recommendations

ABSTRACT: The delivery of active functional molecules across the skin is laborious due to its structural intricacy and exceptional barrier characteristics. Developments in nanotechnology yielded innovative transport vehicles derived from nanomaterials to reinforce the skin's ability to interact with active ingredient molecules and increase its bioavailability. The current study employed crystalline inorganic two-dimensional double hydroxides (LDHs) as an efficient carrier and delivery vehicle for folic acid (FA) in a topical skincare formulation. FA was incorporated into the interlayer region of Mg/Al LDHs utilizing a coprecipitation procedure to produce a nanohybrid. The nanohybrid was characterized by XRD and FTIR. FA intercalation into the interlayer galleries of the nanohybrid was confirmed by an XRD diffractogram, which established a shift of the basal $d_{(003)}$ reflection of LDHs to lower 2θ angles. FTIR of the nanohybrids revealed the characteristic absorption frequencies of FA, indicating the existence of FA within the LDH matrix. The FA-intercalated nanohybrid showed antioxidant activity similar to that of free FA. A topical formulation was prepared by dispersing FA-intercalated LDH nanohybrid in an oil-in-water (o/w) emulsion, and it was used to evaluate its properties further. Rheological property evaluation showed that the presence of the nanohybrid resulted in better flow behavior and higher yield stress of the formulation, implying improved stability and quality. The nanohybrid also enhanced the storage modulus and, thus, the dynamic rigidity of the formulation. The test compounds expressed no cytotoxicity in HaCaT cells, as cell viability significantly increased in monolayer cultures after a 24-h incubation period. Release studies conducted *in vitro* using the nanohybrid showed a pH-dependent controlled release of FA. Transdermal permeation experiments using Franz diffusion cells demonstrated a direct correlation between the concentration of penetrated FA with time, which signified a gradual and effective transfer of FA from the LDH matrix into the oil/water emulsion, demonstrating its efficacy. Thus, the study revealed excellent prospects for the nanohybrid as a multifunctional active ingredient in topical applications.

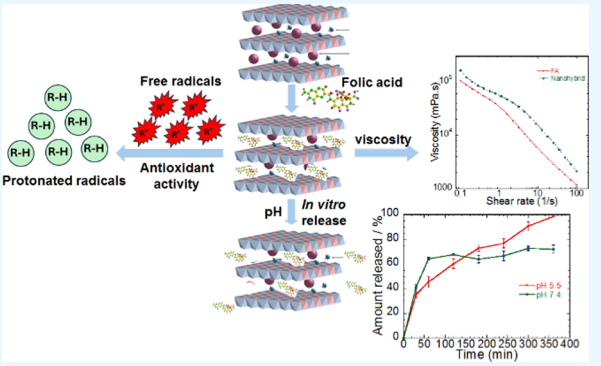

1. INTRODUCTION

Folic acid (FA) is a potent active ingredient in dermal and sun care, with the capacity to combat photoaging and the common signs of aging. It prolongs premature aging of the skin by prompting skin cells, such as fibroblasts, while simultaneously averting DNA impairment.[1] The benefits of FA could also contribute to skin hydration by augmenting the barrier functionality of the skin. Moreover, the concentrations of antioxidants that it contains can decrease the oxidative stress levels on the skin and neutralize damaging environmental free radicals.[2] With the modern demand to maintain skin's natural beauty and texture, FA has been incorporated into personal care and cosmetic skincare formulations.[3,4] The primary disadvantages of the use of FA, particularly in topical formulations, are inadequate solubility as well as susceptibility to UV radiation.[5] The extremely low solubility of FA (1.6 mg/L) in aqueous physiological solutions results in an inhomogeneous dispersion in hydrophilic solvents. Therefore, surfactants, co-surfactants, or co-solvents are used to solubilize FA for consistent formulation. The lack of solubility in organic solvents and less lipophilicity inhibit the infiltration of FA through the skin, while the application of penetration enhancers may weaken the skin barrier. Numerous topical products comprising FA are available commercially for the

Received: June 8, 2024
Revised: November 4, 2024
Accepted: November 8, 2024
Published: November 26, 2024

remediation of aged or photodamaged skin, though the issue of the susceptibility of FA to UV exposure is not considered often.[5] Therefore, it remains necessary to develop innovative strategies for the protection, enhancement of solubility, and controlled release of FA from skincare formulations.

Over the past two decades, there has been a significant focus on hybrid structures, which combine inorganic−inorganic and organic−inorganic elements, due to their unique properties that are not achievable in individual systems.[6−9] This trend has led to rapid growth in the development of bioinorganic nanohybrid systems for the effective topical and transdermal delivery of active ingredients. The continued interest in creating novel topical delivery vehicles is driven by the need to enhance functional activity while minimizing adverse side effects. Bioinorganic nanostructures enable the controlled and safe delivery of numerous bioagents into target sites with great precision. There is a particular demand for the advanced delivery of functional ingredients that are highly sensitive to ambient environments. These hybrid structures must include biocompatible inorganic environments that allow safe retention and the controlled transport of active molecules. Among the various inorganic materials, LDHs stand out as promising inorganic environments due to their unique properties: enhanced dissolution ability, thermal stability, and controlled release of intercalated molecules.[10,11] Their cationic layered framework can encapsulate many biologically essential molecules, such as genes and cosmetic, nutraceutical, or drug molecules.[12−18]

Additionally, the great affinity of LDHs to the carbonate ion and susceptibility to dissolution by acid provide the required release of incorporated drugs as well as compatibility and multifunctionality with various biosystems.[13] A thorough search of the data available in the relevant literature shows that the properties of FA-intercalated LDH nanohybrids have been predominantly investigated in their neat form (without being incorporated in a formulation). Moreover, only a few properties were evaluated in the few cases where nanohybrids have been incorporated into a formulation. Hence, the current study was designed to fill this gap and demonstrate the multifunctional properties of the FA-intercalated LDH nanohybrids incorporated in a topical formulation. This study is a significant contribution to the field, as it provides valuable insights into the potential of these nanohybrids as a topical delivery system for FA. An FA-intercalated Mg/Al LDH nanohybrid material was prepared, and it's *in vitro* release (neat nanohybrid) and transdermal diffusion (nanohybrid formulation) properties as a prospective topical delivery system were investigated. Furthermore, the study sought to evaluate the antioxidant functionality of the hybrid material. The cytotoxicity of the prepared hybrid material was assessed by monitoring the cell viability and proliferation of HaCaT in its presence.

2. MATERIALS AND METHODS

2.1. Materials. Reagents and chemicals were utilized as obtained, unless stated otherwise. Aluminum nitrate nonahydrate (ACS reagent, $Al(NO_3)_3{\cdot}9H_2O$, 98% purity) and magnesium nitrate hexahydrate (ACS reagent, $Mg(NO_3)_2{\cdot}6H_2O$, 98% purity) were obtained from Sigma-Aldrich, Johannesburg, South Africa. FA was acquired from Protea Laboratory Solutions, Johannesburg, South Africa. Sodium hydroxide (NaOH) was acquired from MINEMA Chemicals, Johannesburg, South Africa. PBS (pH 7.4) solutions, crucial for maintaining the physiological pH during the experiment, were prepared by using a well-known literature procedure. Nylon membrane filters with a 0.45 μm pore size were employed for transdermal diffusion testing. The ingredients for the preparation of o/w emulsions such as mineral oil, emulsifiers (cetearyl alcohol, stearic acid, glyceryl stearate, and PEG-100 Stearate), glycerol, and phenoxyethanol were kindly supplied by Amka Products Pty Ltd., Pretoria, South Africa.

2.2. Synthesis of FA-Intercalated Mg/Al LDH Nanohybrid. A coprecipitation method, adopted from our previous work with minor alterations,[19] was used to synthesize the FA-intercalated Mg/Al LDH nanohybrid. Typically, suitable amounts of $Mg(NO_3)_2{\cdot}6H_2O$(0.05 mol) and $Al(NO_3)_3{\cdot}9H_2O$ (0.025 mol) were dissolved in decarbonated deionized water in a 250 mL beaker at 85 °C while purging with N_2 gas. An FA solution (0.025 mol) in 2 M NaOH was added dropwise to the vigorously stirred solution. With the temperature maintained at 85 °C and constant N_2 gas purging, a 2 M NaOH solution was added dropwise until the yellow/red suspension was maintained between pH 9 and 10. The solution was mixed under these conditions for 2 h and then aged at room temperature (25 °C) for 72 h. The yellow/orange precipitate attained was then filtered, washed numerous times using deionized decarbonated water, and subsequently dried in a vacuum oven at 50 °C for 24 h. The nanohybrid was pulverized, sieved to pass through a 75 μm sieve, and enclosed in a vessel for more experiments and analyses. The neat Mg/Al LDH nanostructure was synthesized by using the same method in the absence of FA.

2.3. Characterization. The X-ray diffractometer with Cu Kα-radiation (1.5406 Å) at 40 mA and 45 kV (PANalytical X'Pert PRO, Netherlands) was employed to obtain the XRD patterns of the nanohybrid and unmodified Mg/Al LDHs. XRD spectra were acquired using a step size of 0.02° and a scan rate of 2°/min in the 2θ range of 0 to 40°. The vibrational characteristics of the samples were investigated by a Spectrum 100 attenuated total reflectance Fourier transform infrared spectrometer (ATR-FTIR, PerkinElmer) using eight scans, 4 cm^{-1} resolution, and 4000−500 cm^{-1} wavenumber range. Thermal degradation profiles of Mg/Al LDHs and FA-nanohybrids were attained through thermogravimetric analysis using a TGA Q500 (TA Instruments) in the air atmosphere. The FA loading efficiency of Mg/Al LDH was assessed using a Lambda 70s UV−Vis spectrometer (PerkinElmer).

2.4. Determination of FA Loading. The FA loading efficiency of Mg/Al LDH was evaluated using UV−Vis spectrometry after the complete dissolution of the nanohybrid.[19] In a typical experiment, 50 mg of nanohybrid was dissolved in a 1:1 mixture of HCl (1 M)/DMSO (100 mL). UV−Vis spectrophotometry (Lambda 70s, PerkinElmer) at a wavelength of λ = 296 nm was used to determine the concentration of FA in the solution. A stock solution of FA in DMSO (100 ppm) was used to prepare the calibration standards by diluting suitable volumes in 50 mL of DMSO. Each experiment was performed in triplicate, and the mean values were presented.

2.5. DPPH Antioxidant Assay. The antioxidant property of the nanohybrid was evaluated by 1,1-diphenyl-2-picrylhydrazyl (DPPH) assay as described by Mavundza et al.[20] with slight alterations in 96-microwell plates. The working concentration range for the nanohybrid and reference FA was from 250 to 16,000 μg/mL in DMSO. To these 100 μL suspensions, 100 μM DPPH solution (100 μL) was added,

https://doi.org/10.1021/acsomega.4c05374
ACS Omega 2024, 9, 48185−48195

followed by incubation in the dark for 30 min at room temperature (25 °C). The radical scavenging capacities were measured using a multiwell plate reader (Hidex Sense Beta, South Africa) at a wavelength λ = 517 nm for 2 h with DMSO as a blank. The absorbance values were corrected by subtracting the absorbance of the dispersed LDH particles. The average of triplicate measurements of the effective sample concentration to decrease the initial DPPH absorbance by 50% (EC_{50}) was presented as a measure of the free radical scavenging property.

2.6. Cytotoxicity Assay. *2.6.1. Culturing of HaCaT Cells.* Human keratinocyte (HaCaT) cells were provided by the Department of Pharmacology, University of Pretoria, South Africa. HaCaT cells were grown in T75 flasks (Corning Cell-99 BIND, Corning, NY) containing Dulbecco's modified eagle medium (DMEM) with 10% heat-inactivated fetal bovine serum (FBS) and 1% antibiotics (100 U/mL penicillin, 100 μg/mL streptomycin, and 250 μg/mL fungizone) (Gibco-Life Technologies, South Africa) at 37 °C in a humidified incubator set at 5% CO_2. The replacement of the growth medium was performed every 48−72 h. Confluence was estimated by observing under a Zeiss AxioCam Primo Vert inverted phase-contrast microscope (Carl Zeiss, Germany).

2.6.2. Subculturing of HaCaT Cells. HaCaT cells were detached using trypsin-ethylenediaminetetraacetic acid (EDTA) once they had reached 80 to 90% confluence. Old complete DMEM was aspirated from the T75 culture flasks. Cultures were rinsed with phosphate-buffered saline (PBS) and chemically detached using trypsin-EDTA (0.25% trypsin containing 0.01% ethylenediaminetetraacetic acid (EDTA)) for 10 min at 37 °C. Cells were centrifuged at 1500 rpm for 5 min (Beckman Coulter, Germany) after being transferred into a centrifuge tube (15 mL). The supernatant was discarded, and the pellet of cells was resuspended in 1 mL of 10% FCS-supplemented medium. This suspension was partitioned into separate flasks containing preheated culture medium at a ratio of 1:15, and the flasks were reincubated. The cells were enumerated by utilizing a trypan blue dye exclusion method, seeded, and grown with or without the test samples at various concentrations. Cells exposed to the medium without active ingredients were used as positive controls.

2.6.3. MTT Cytotoxicity Assay. The test samples, FA and nanohybrid (amount equivalent to 1 mg of FA), were added to 5 mL of DMEM, vortexed, and incubated for 2 h at 37 °C. HaCaT cells were seeded into clear, sterile, flat-bottom 96-well plates (1×10^4 cells/mL) and incubated for 24 h for cellular attachment. Upon the cells reaching a confluence of 80−90%, they were washed with fresh DMEM. Subsequently, the cells were exposed to 100 μL of the serial dilutions of FA and nanohybrid test samples. The HaCaT cells were treated with serial dilutions of FA and nanohybrid at 0.001, 0.002, 0.004, 0.008, 0.016, 0.031, 0.063, 0.125, 0.25, 0.5, and 1 mg/mL: n = 9. The FA and nanohybrid test samples, as well as their serial dilutions, were added to every well and further incubated in a humidified incubator (5% CO_2 atmosphere for 24 h at 37 °C). The viability of cells was evaluated by the reduction of 3-(4,5-dimethylthiazol-2-yl)-2,5-diphenyltetrazolium bromide (MTT) (5 mg/mL) to formazan. After 24 h, 10 μL of MTT was poured into the wells with incubation for 4 h at 37 °C in a CO_2 incubator. 100 μL of SDS-HCl solution was poured into each well, and incubation was continued for a further 4 h to confirm the complete dissolution of the formed formazan crystals. The absorbance was measured at a wavelength λ = 570 nm in a microplate reader (Tecan Infinite 500, LifeScience). The viability of cells was recorded as a percentage of that of the negative control. Absorbance was used as a measure of the cell viability and cytotoxicity. Reduction of the cell viability was employed as a measure of keratinocyte toxicity.

2.7. *In Vitro* Release Study. Experiments were conducted at two pH values (pH 5.5 and 7.4) to measure the quantity of intercalated FA released from the Mg/AL LDH matrix, as described in our previous study.[19] 50 mg of nanohybrid was mixed with 100 mL of PBS in a polyethylene bottle. The bottle was agitated at 75 rpm in a constant temperature water bath (25 ± 1 °C). Samples were removed (5 mL) at regular intervals, initially after 30 min and then at 60 min intervals for 6 h. To maintain a constant volume, the sample withdrawn was replenished with an equal volume of PBS (5 mL) at the same pH. The absorbance of released FA from the nanohybrid was measured at a wavelength of 280 nm by a UV spectrometer (Lambda 70s, PerkinElmer). For the experiments at pH 5.5, the pH of PBS was adjusted from pH 7.4 to 5.5 using 0.1 M HCl. The results were presented as the mean values of triplicate measurements.

2.8. Preparation of Topical Formulations. An oil/water (o/w) emulsion (cream formulation) prepared with Mg/Al-FA was used to assess the permeation characteristics of FA from the nanohybrid.[20] The water and oil phases for the preparation of the emulsion were put together using the constituents, as presented in Table 1. Each phase was separately heated to 75 °C in a vessel. The oil phase was steadily poured into the water phase under dynamic stirring. The emulsion was exposed to high-shear homogenization using a high-shear mixer (IKA T25 shear mixer, IKA, Germany) at 6000 rpm for 3 min. After cooling the emulsion below 40 °C, a preservative was added, and subsequently, the pH was adjusted to 5.5. The formulations were stored in polypropylene bottles at room temperature (25 °C) for further analyses.

Table 1. Ingredients and Input Rate for the Preparation of the Cream Formulation

ingredient	wt %	
	Mg/Al-FA cream	FA cream
Aqueous Phase		
water	to 100	to 100
glycerin	5	5
xanthan gum	0.3	0.3
Mg/Al-FA nanohybrid	5	0
folic acid	0	1.05
Oil Phase		
mineral oil	5	5
stearic acid	1	1
glyceryl stearate/PEG-100 stearate	3	3
cetearyl alcohol	4	4
preservative	0.5	0.5
pH adjuster	q.s.	

2.9. Rheology Measurements. The rheological characteristics of the FA and nanohybrid formulations were assessed by an MCR501 rheometer (Anton Paar) equipped with parallel plate geometry (PP50s) with an adjusted gap of 1 mm. The sample was placed centrally on the stationary plate. Flow curves were obtained under rotational rheology mode with a stepwise increase of shear rate ranging from 0.01 to 100 s^{-1} at 27 °C. The amplitude sweep (strain ranging from 0.01 to

https://doi.org/10.1021/acsomega.4c05374
ACS Omega 2024, 9, 48185−48195

100%) with a preadjusted angular frequency of 6.28 rad s^{-1} was used to determine the linear viscoelastic region (LVE) of the cream formulations at 27 °C.

2.10. *In Vitro* Franz Cell Diffusion Experiments. The skin permeation experiments were conducted utilizing an HDT1000 Franz diffusion cell (Copley Scientific) with a 12 mL capacity.[19] The vertical diffusion system was equipped with an integrated heating block and a magnetic stirrer. The receptor compartment was filled with PBS (pH 7.4) and kept at a constant temperature (32 °C). The donor and receptor chambers were separated by placing a synthetic membrane made of nylon (pore size = 0.45 μm). The test formulation (~0.3 g) was placed in the donor compartment. Three mL of samples were withdrawn from the receptor compartment at regular intervals, initially after 30 min and afterward at 60 min intervals for 6 h. Each withdrawn sample was instantly replaced with an equal amount of PBS to conserve a constant volume. The concentration of FA permeated through the membrane was analyzed using a UV spectrometer at wavelength λ = 280 nm. The average values of triplicate measurements represented the results.

3. RESULTS AND DISCUSSION

3.1. FA-Intercalated Mg/Al LDH Nanohybrid Characterization. The unmodified LDH and nanohybrid were synthesized using the coprecipitation approach (low supersaturation). The resulting samples were subjected to a rigorous analysis on the FTIR, TGA, and XRD, ensuring the utmost accuracy in verifying whether FA intercalated into Mg/Al LDH.

The integration of FA into the interlayer spaces of Mg/Al LDH was ascertained using an X-ray diffraction technique, and the diffraction patterns of pristine Mg/Al LDH and the nanohybrid are reported in Figure 1. The XRD pattern of Mg/Al LDH showed a reflection at an angle of 2θ = 10.54° (basal spacing $d_{(003)}$ = 8.37 Å), which was due to intercalated NO_3^- ions. These values agree with those reported by Choy et al.,[6] Pagano et al.,[21] Qin et al.,[22] Cao et al.,[23] as well as Roy et al.,[24] for a pristine Mg/Al(NO_3) LDH, thereby validating our findings. In the diffraction pattern of the nanohybrid, a new reflection appeared at an angle 2θ = 4.82° (basal spacing $d_{(003)}$ = 18.30 Å) with a clear disappearance of the reflection at 2θ = 10.54°. Choy et al.[6] and Pagano et al.[21] also observed a similar basal spacing $d_{(003)}$ value (19.1 Å) for the nanohybrid. The disappearance of the 2θ = 10.54° reflection and the emergence of the 2θ = 4.82° reflection indicated successful intercalation of FA into the interlayers of Mg/Al LDH. Determining the height of the interlayer space of the FA-intercalated Mg/Al LDH nanohybrid by deducting the thickness of the brucite layer (4.8 Å) allowed for the prediction of the orientation of the FA molecules in the interlayer spaces of Mg/Al LDH. It was determined that the FA molecules were organized in a sloped longitudinal monolayer with slanting angles of 45.6°—a similar observation to a previous report.[1] These observations indicated that FA anions (folate) replaced the NO_3^- ions and, thus, have been inserted into the interlayer galleries of the Mg/Al LDH nanohybrid.

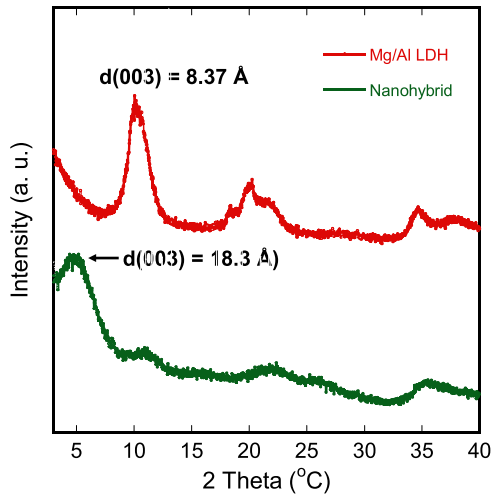

Figure 1. X-ray diffraction spectra of Mg/Al LDH, nanohybrid, and FA.

Figure 2 illustrates the ATR-FTIR spectra of FA, nanohybrid, and pristine Mg/Al LDH. FTIR spectra exhibited the typical vibration frequencies for pristine Mg/Al LDH and FA. For the pristine LDH, a broad signal centered at 3415 cm^{-1} (Figure 2a) was ascribed to the hydroxyl (OH) group stretching frequency of intercalated H_2O molecules and the brucite-like layers of Mg/AL LDH.[6,21−28] The peak appearing at around 1642 cm^{-1} was ascribed to the distortion or bending frequency of H_2O in the interlayers of the LDH. The signal observed at 1347 cm^{-1} was attributed to the asymmetric stretching ν_3 mode of the NO_3^- ions, demonstrating the existence of NO_3^- in between the layers of Mg/Al LDH. However, the asymmetric stretching mode ν_3 usually appears around 1380 cm^{-1}.[6,21−28] Upon incorporation of FA into the interlayers of Mg/Al LDH, the signal associated with the NO_3^- ions disappeared. This indicated that FA anions in the nanohybrid replaced most of the NO_3^- ions. Various signals observed on the spectrum of the nanohybrid were mostly attributed to the presence of FA (Figure 2b). As such, the band that appeared at 1410 cm^{-1} was accredited to the stretching vibrations of −NH− of the pterine and *p*-aminobenzoic acid moieties,[29−31] and the band appearing at 1452 cm^{-1} was credited to the C=C bond stretching vibration of the aromatic ring backbone.[1] The band observed at 1182 cm^{-1} was attributed to the C−N bond vibrations.[27,30] The other bands that appeared on the Mg/Al-FA (1337, 1107, 835, and 762 cm^{-1}) corresponded with the bands in the spectrum of FA.[27] This information obtained from FTIR spectra unequivocally confirms the formation of an FA-intercalated Mg/Al LDH matrix hybrid or nanohybrid.

The thermal degradation of Mg/Al LDH and the nanohybrid was investigated using a thermogravimetric analyzer, and their thermal degradation profiles are depicted in Figure 3. The first thermal event (T_1) in the thermograms of Mg/Al LDH and nanohybrid appeared between 0 and 200 °C, depicting the loss of adsorbed water molecules.[1,25−29] The second thermal event (T_2) for Mg/Al LDH occurred between 200 and 300 °C—the loss of interlayer water molecules—appeared to have overlapped with the third thermal event (T_3) between 300 and 500 °C, which was accounted for the onset of loss of water molecules through dehydroxylation.[28−30] The second thermal event (T_2) for the nanohybrid was observed between 200 and 300 °C, indicating the loss of interlayer water molecules. Furthermore, the third thermal event (T_3) for the nanohybrid appeared between 300 and 400 °C. This thermal event is attributed to the degradation of FA molecules.[1,25−29] In the fourth thermal event (T_4), at around 500 °C, Mg/Al

https://doi.org/10.1021/acsomega.4c05374
ACS Omega 2024, 9, 48185−48195

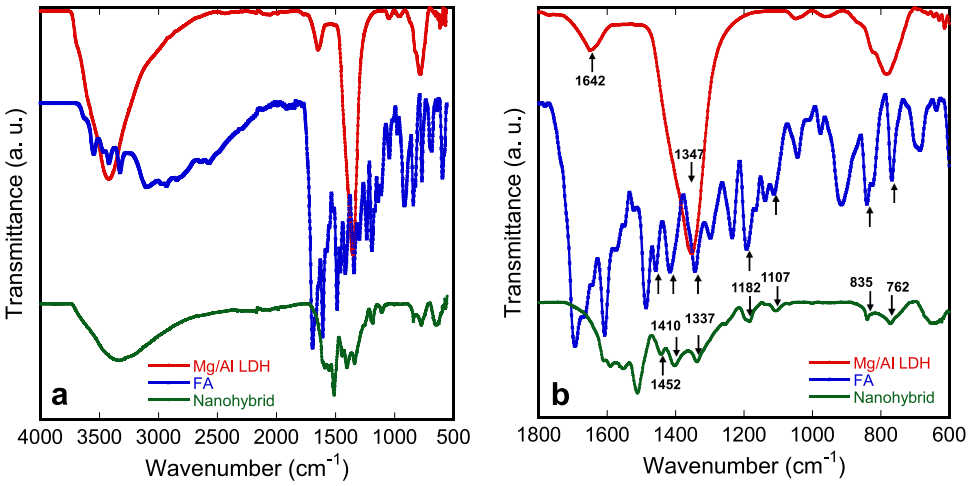

Figure 2. FTIR spectra of FA, Mg/Al LDH, and the nanohybrid: (a) full range and (b) expanded range.

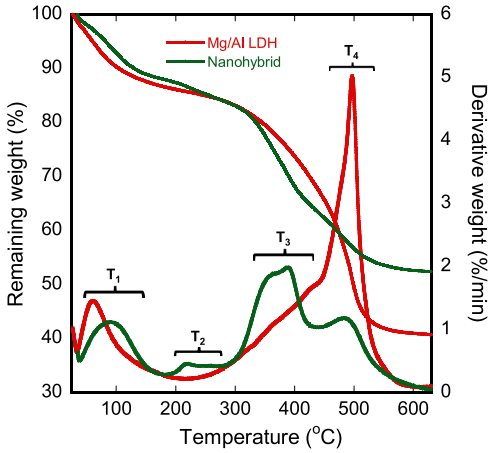

Figure 3. Thermal degradation profiles of Mg/Al LDH and the nanohybrid.

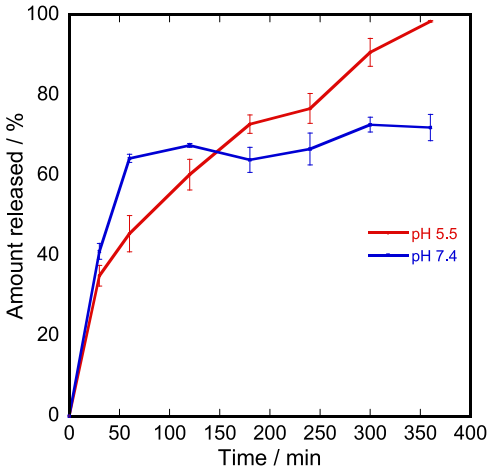

Figure 4. *In vitro* release profile of FA from nanohybrid at pH 5.5 and 7.4.

LDH and the nanohybrid exhibited a narrow high-intensity and a broader low-intensity signal, respectively. These signals indicated further structural collapse due to dehydroxylation.

3.2. Loading of FA into Nanohybrid. Before exploration of the release profile and the skin permeation of FA from the nanohybrid, the FA loading into the Mg/Al LDH interlayers was verified. The amount of FA loaded was assessed by the dissolution of a known mass of nanohybrid (50 mg) in 50 mL of 1 M HCl in DMSO. The resulting solutions were analyzed by UV−Vis spectrometry. The loading of FA into Mg/Al LDH to form a nanohybrid was determined to be 21.1 ± 0.2%. These findings correspond to those Qin et al.[25] disclosed for loading FA into a Mg/Al LDH. However, higher loadings of FA into Mg/Al LDH have been reported in other studies.[21,25,27]

3.3. *In Vitro* Release Study. Exploratory *in vitro* release experiments were carried out to evaluate the release profile of FA anions from Mg/Al LDH nanohybrid in PBS media at different pHs of 5.5 and 7.4. Figure 4 presents the release of FA from the nanohybrid at 32 °C for 6 h at the chosen pH values. After the first 60 min, it was observed that FA ions were rapidly released into the receptor medium for both pH 5.5 and 7.4. The rapid (burst) release in both pH environments was attributed to the release of surface-adsorbed anions because of weak electrostatic connections with the LDH surface[27,32,33] and some FA ions in the interlayer space of the nanohybrid.[34,35] The quantity of FA ions released initially at pH 4 was much higher than that released at pH 5.5, with the amount released after 60 min at pH 7.4 (64%) being 1.4 times more than that released at pH 5.5 (45%). This rapid release was succeeded by a slower release of FA ions, indicated by the slope change, after 30 and 60 min for pH 5.5 and 7.4, respectively. It was suggested by Gu et al.[36] that the dual-phase and constant release properties could perform an imperative part in the bioavailability of the ingredient, as the first burst release presents the necessary quantity, and the succeeding extended release sustains the quantity over a lengthy period. Elsewhere, it has also been detailed that the inflexibility of the LDH layers, as well as the distance of the diffusion path, modulate the diffusion of organic anions in LDH.[37] This lower release of FA at pH 5.5 was ascribed to insufficient solubility of FA between pH 1 and 7[38] and the strong buffer effect of nanohybrid at low pH values.[22,27] This phenomenon has also been observed previously, where the release of a drug molecule from the LDH hybrid was more at pH 7.2 than at pH 4.8.[39,40] In another study, the release of an anionic drug from the nanohybrid at pH 4 was nearly equal to that at pH 7.[41] A plausible elucidation for what was observed at pH 5.5 could be that with PBS at slightly acidic pH, phosphate ions largely exist

https://doi.org/10.1021/acsomega.4c05374
ACS Omega 2024, 9, 48185−48195

as $H_2PO_4^-$ molecules which, after the interaction with the OH groups of the Mg/Al LDH layers, create a layered Mg/Al hydroxyphosphate.[40−42] In this fixed state, the strongly attached phosphates are unexchangeable, preventing the diffusion of intercalated FA anions.[38] At pH 7.4, the PBS comprises both the $H_2PO_4^-$ and HPO_4^{2-} molecules.[40−42] HPO_4^{2-} molecules interact with the OH groups of LDH only when dehydration over P_4O_{10} occurs or above 40 °C.[40−42] Furthermore, the $H_2PO_4^-$ concentration at neutral pH (pH 7.4) is lesser than at slightly acidic pH (pH 5.5), resulting in reduced grafting and less hindrance of the intercalated FA diffusion, with HPO_4^{2-} molecules being involved in ion exchange with FA anions. FA's lengthier release rate (change of gradient) until 30 min at pH 5.5 could result from the phenomenon described above.[40,41] As was anticipated, the quantity of FA anions released after 150 min at a slightly acidic pH (pH 5.5) was higher than that at pH 7.4. Upon the release of FA adsorbed on the LDH surface, the outcome of the disruption of the structure of the LDH under acidic conditions became apparent as more FA anions were released at pH 5.5 than at pH 7.4. After 60 min, a steadier release of FA ions was observed at pH 7.4, while the release at pH 5.5 was faster. However, the quantity of FA released at pH 7.4 continued to be more significant compared with pH 5.5 until 150 min, where a crossover was observed. Beyond 150 min, the quantity of released FA remained higher at pH 5.5 than at pH 7.4. This implied that the FA anion release at pH 5.5 was driven by both the dissolution of the Mg/Al-FA as well as the exchange of intercalated FA ions with phosphate ions. The maximum amount of FA ions released at pH 5.5 and pH 7.4, after 360 min, was 98.4 and 72%, respectively. Thus, these results indicated that at the physiological pH of the skin (pH 5.5), more FA will be released, leading to enhanced bioavailability and improved formulation efficacy.

3.4. DPPH Antioxidant Assay. The DPPH oxidative assay was used to determine the antioxidant activities of FA and the nanohybrid *in vitro*. The stable DPPH free radical is generally used to evaluate the potential of the materials to perform as scavengers of free radicals. The decrease in absorbance of the DPPH free radical at wavelength λ = 517 nm due to proton donation by the FA indicates antioxidant activity.[25,35] Figure 5 depicts the antioxidant activity of FA and the nanohybrid against the DPPH free radical after a reaction time of 90 min.

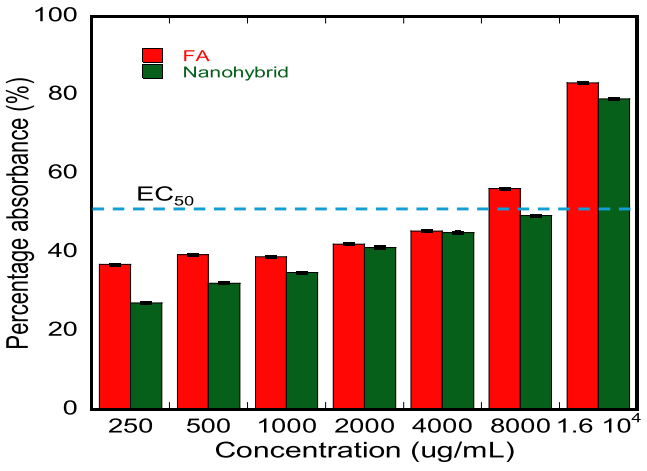

Figure 5. Antioxidant activity of FA and the nanohybrid at different concentrations after 90 min.

It was apparent that the antioxidant activity was dependent on concentration. The maximum absorbance reduction for FA and nanohybrid was observed at 2133 μg/mL, and it was 83.1 and 79%, respectively. At 1067 μg/mL concentration, the absorbance reduction was 56.2 and 49.3% for FA and nanohybrid, respectively. Thus, this concentration was considered to be effective (EC_{50}) for both FA and the nanohybrid. This indicated that there was not much difference in the antioxidant activity between free FA and the nanohybrid. These results illustrated that FA maintains its integrity and antioxidant functionality even after the intercalation into LDH. The phenomenon of similar antioxidant activities between antioxidant compounds and their LDH-intercalated hybrids has been reported previously for 3-(3,5-di*tert*-butyl-4-hydroxyphenyl)-propionic acid (BHPPA) and gallic acid.[43,44] However, at lower concentrations (250 and 500 μg/mL), a substantial difference was observed in the antioxidant activity between free and phenolic acid−intercalated LDH. This was attributed to the lag in the antioxidant activity of nanohybrids, as the DPPH molecules had to diffuse into the interlayers of the LDH before they interacted with the intercalated phenolic acid.[43,45] It is worth noting that Qin et al.[25] had a different observation from the current study; they reported that the Mg/SL LDH-FA hybrid displayed better antioxidant activity than the free FA. Unfortunately, in the work by Qin et al.,[25] the information about the EC_{50} of both FA and its LDH hybrid was not provided.

3.5. *In Vitro* Cytotoxicity Assay. HaCaT cells exhibited the typical morphology of keratinocytes under 2D single-layered tissue growth conditions. For *in vitro* cytotoxicity testing, monolayer cell culture systems were used to assess the system's suitability. The 2D HaCaT cell lines were treated with test materials and then incubated for 24 h to stimulate a potential skin toxicity environment. *In vitro* cytotoxicity assays were performed to assess and delineate the capability of the test samples and to determine the safety of using nanohybrids in topical skincare. Therefore, the effect of FA and its nanohybrid on the viability of immortalized keratinocyte cells was evaluated.

Analysis of the cellular morphology displayed the cellular reaction of single-layered HaCaT cells against FA and the nanohybrid. The test compounds expressed no significant cytotoxicity on HaCaT cells; cell viability was significantly proliferated in monolayer cultures after a 24-h incubation period (Figure 6).

The development of epidermal model systems is essential for assessing skin irritation, as well as the viability of cells, healing of wounds, and toxicity. Compared with basic cell cultures, HaCaT cell cultures present more dependable sources of keratinocyte cells. Inflammatory reactions and cytokine release differ when HaCaT cell cultures are dosed with various concentrations of FA, which indicates that they are suitable as a skin-related pathology model.[46,47]

3.6. Rheological Behavior of Formulations. In steady-state rheology measurements, samples are subjected to incremental rotational shear, and the sample viscosity is computed as a shear rate function. The rheograms so acquired denote the flow behavior of the sample across a broad scale of shear rates. This mimics the semisolid behavior under various environments, i.e., the lower shear rates mimic a stationary sample, and high shear rates mimic a sample when applied.[48] Figure 7a presents the steady-state flow properties of formulations containing neat FA and the nanohybrid. The

https://doi.org/10.1021/acsomega.4c05374
ACS Omega 2024, 9, 48185−48195

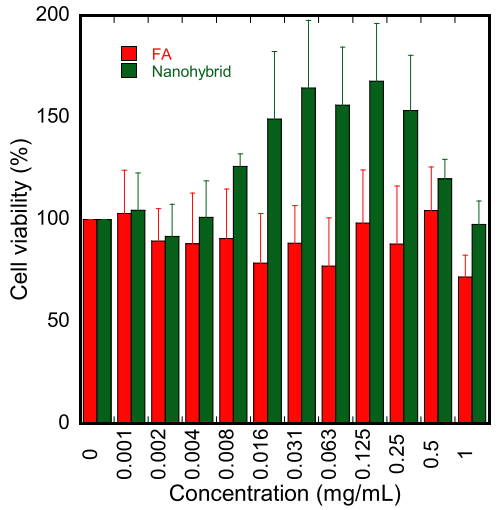

Figure 6. Effect of HaCaT keratinocyte viability when exposed to different amounts of test formulations in DMEM derived from FA (green) and nanohybrid (green) (n = 9).

flow curves exhibited non-Newtonian flow behavior with a significantly higher viscosity in the region of 10^5 mPa s at the low shear rate for both formulations, with the viscosity of the nanohybrid formulation being higher than that of neat FA (Figure 7a). This result agrees with a report by Pagano et al.,[5] who observed that FA-intercalated LDHs (Zn/Al and Mg/Al) increased the viscosity of emulsion gels. Moreover, these organically modified LDHs, particularly the nanohybrid, improved the flow capacity of the emulsion gels. This result indicated that the nanohybrid could function as a thickening agent.

The shear viscosity progressively diminished with an increasing rate of shear, illustrating a shear thinning behavior, which is the general flow behavior of most cosmetic emulsions.[49−51] A higher yield stress value (16.2 ± 25 Pa) was also observed for the nanohybrid formulation, which could be attributed to the 2D platelet structure of LDH that exhibited resistance to the flow. In contrast, the neat FA formulation showed a lower yield stress of 11.6 ± 1.53 Pa. Brummer et al.[52] reported that the high initial viscosity and yield stress in formulations signify longer ingredient shelf life and stability during storage. The stability of an emulsion is usually predicted by Stokes' equation (eq 1), which relates to the settling rate of the dispersed oil droplets with viscosity and the droplet size:[53]

$$V = \frac{2gr^2(\rho - \rho_0)}{9\eta} \quad (1)$$

where V is the settling rate, r is the droplet radius, ρ is the droplet density, ρ_o is the dispersion medium density, η is the bulk phase viscosity, and g is the gravity. Equation 1 illustrates that the settling velocity of an emulsion can be decreased by a highly viscous continuous phase, resulting in an increased emulsion stability. The findings of the current study showed that the nanohybrid could improve the stability of the formulation as it increases the viscosity of the bulk (water) phase.[54]

In dynamic rheology studies, oscillatory stress at small strains (0.01−100%) is applied to the sample while the angular frequency (6.28 rad·s^{-1}) is kept constant to measure viscoelastic properties.[48] Figure 7b showed a higher storage modulus (G') for the formulation containing nanohybrid when compared to the corresponding neat FA formulation, showing superior elasticity, indicating a powerful dynamic inflexibility (rigidity) of the emulsion.[55,56] This indicated a predominance of solid-like behavior and the potential of the formulation for elastic energy storage due to the presence of LDH particles.[57] This result was consistent with the report by Perioli and co-workers[58] as they observed higher concentration-dependent storage modulus (G') values for gastric mucus containing LDH intercalated with retinoic acid. These results indicated that the nanohybrid can enhance topical formulations' stability and flow behavior.

3.7. Skin Permeation Studies. When an active ingredient in a cosmetic formulation is smeared on the skin surface, two successive physical processes become rate-limiting steps in skin permeation—the active ingredient released from the carrier and its diffusion through the skin barricade.[59] Thus, the capability of FA to permeate through the skin layers was investigated with Franz vertical diffusion using a cream formulation containing nanohybrid. Synthetic nylon membrane filters with 0.45 μm pore size were employed as a barrier between the receptor and donor media, and PBS (pH 5.5 and 7.4) was used as a receptor medium. The flux (J_{ss}, μg·cm^{-2}·h^{-1}) in the steady-state and the permeation coefficient (K_p, cm·

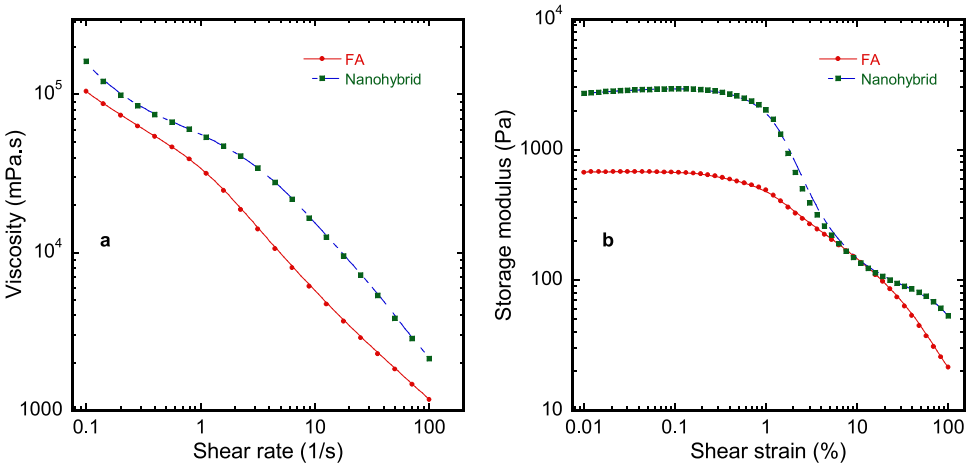

Figure 7. Rheological properties of FA and the nanohybrid formulations: (a) flow curves and (b) amplitude sweep curves.

https://doi.org/10.1021/acsomega.4c05374
ACS Omega 2024, 9, 48185−48195

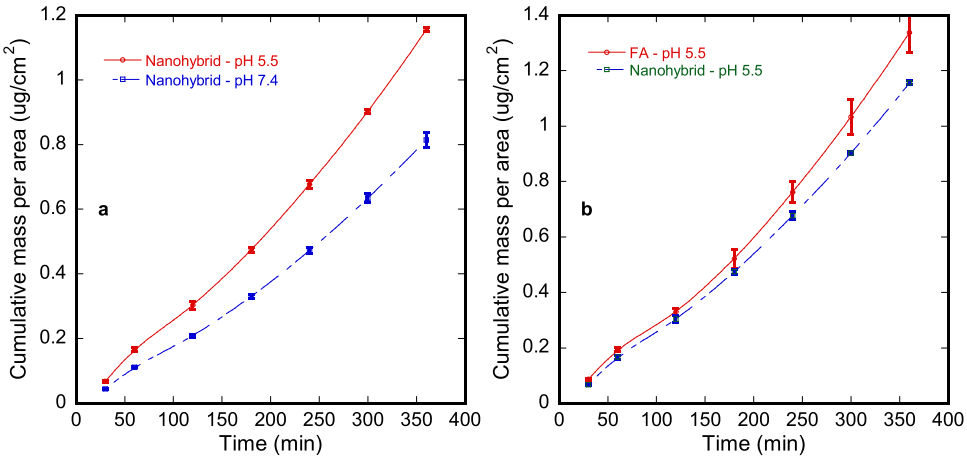

Figure 8. Plots of cumulative amount permeated per area vs time for (a) nanohybrid-based formulations at different pH values. (b) FA and nanohybrid formulation at pH 5.5.

h^{-1}) were determined by plotting the cumulative concentration of FA permeated per area against time (Figure 8a). The value of J_{ss}, the steady-state flux, was determined from the gradient of the linear region of the curve, while the permeability coefficient, K_p, was calculated by dividing the flux by the mass of FA used in the cream. The calculated permeability parameter values (J_{ss} and K_p) at pH 5.5 and 7.4 are depicted in Table 2. The steady-state flux and the permeability coefficient

Table 2. Permeation Parameters for FA and Nanohybrid Formulations at Different pH Values

sample	pH	flux (J_{ss}) ($\mu g \cdot cm^{-2} \cdot h^{-1}$) $\times 10^{-2}$	coefficient of permeability (K_p) ($cm \cdot h^{-1}$) $\times 10^{-5}$
FA	5.5	7.0	2.1
		6.0	1.9
nanohybrid	7.4	4.2	1.3

at pH 5.5 were 6.0×10^{-2} $\mu g \cdot cm^{-2} \cdot h^{-1}$ and 1.9×10^{-5} $cm \cdot h^{-1}$, respectively. The permeability parameters at pH 5.5 for the nanohybrid were significantly higher than those at pH 7.4, where the steady-state flux and permeability coefficient were 4.2×10^{-2} $\mu g \cdot cm^{-2} \cdot h^{-1}$ and 1.3×10^{-5} $cm \cdot h^{-1}$, respectively. The higher penetration of FA from the formulation containing Mg/Al-FA at pH 5.5 than at pH 7.4 was expected, as already shown above (*in vitro* release of FA from neat Mg/Al-FA). The consequence of changing the pH of the medium on the drug release characteristics of LDHs was demonstrated in the work of Mallakpour and Hatami.[60] The synthesized LDH hybrids, Mg/Al-FA, and Mg/Al-FA/chitosan beads, were added to a tea bag and sequentially immersed in buffer solutions with pH 1.2 for 2 h, pH 6.8 for 2 h, and pH 7.4 for 4 h. The release of FA from the nanohybrid was higher in the acidic than in the basic medium. The observations in the current study are consistent with those reported by Mallakpour and Hatami,[60] as permeation of FA from Mg/Al-FA was superior at pH 5.5 to that at pH 7.4.

Therefore, this result ascertains that the nanohybrid could be suitable for the preparation of topical formulations and that the environment (pH 5.5) could ensure the release of FA in a sustained manner. Further comparison of the transdermal diffusion performance of the formulation containing nanohybrid was conducted against that containing neat FA. The comparison experiments were performed at pH 5.5, since cosmetic formulations are traditionally prepared for the physiological pH of the skin (pH 5.5). The formulation containing neat FA appeared to have a similar penetration of FA than that containing Mg/Al-FA until 120 min (Figure 8b). The amount of penetrated FA from the formulation containing neat FA and that containing the nanohybrid after 120 min was 9.9 and 9.6%, respectively. This could be attributed to the fact that the bulk of FA released from nanohybrid, initially, was the surface-adsorbed[26] as well as some intercalated FA.[36] Beyond 120 min, the amount of penetrated FA from the formulation containing neat FA became slightly higher than that containing Mg/Al-FA, with the amount of FA penetrated being 71.2 and 64.4%, respectively, after 360 min. Xiao et al.[26] observed 67% initial release of FA after 25 min for FA-intercalated ternary Mg/ZnAl LDH, which was attributed to the higher concentration surface-adsorbed FA. However, after incorporating it into a formulation, the authors did not investigate the release behavior of FA-intercalated LDH. The study by Gu et al.[36] reported a gradual and biphasic release of low molecular weight heparin (LMWH) anions with an initial burst release of 20.3% from a Mg/Al LDH after 12 h, which was succeeded by a slower LMWH release after 120 h (44.7%). Further observations revealed a slow dissolution of the LDH at pH 7.4, which accounted for the release of LMWH in the initial release stage.[36] Table 2 depicts the permeation parameters for the formulations containing FA and nanohybrid. Pagano et al.[5] performed a comparative transdermal diffusion study between three emulsion gels—(i) containing neat FA (control), (ii) containing a physical blend of FA and Mg/Al LDH, and (iii) containing nanohybrid in sweat medium (pH 5.5). They observed that the emulsion gel formulation containing nanohybrid exhibited much slower permeation of FA than the emulsion gel containing neat FA. The observation was attributed to two aspects: the active molecules' release kinetics from the nanohybrid and the influence of the polymer network present in the aqueous emulsion phase. The results of this study can be claimed to agree with those of Pagano and coworkers.[5] However, the permeation of FA from the formulation nanohybrid was slightly slower than from the formulation containing neat FA. In an earlier study, a nanohybrid material was reported to release FA slower than the physical blend of FA and Mg/Zn/Al LDH at pH 7.4.[27] However, unlike in this study, the materials were not incorporated in any matrix (formulation) before evaluation

https://doi.org/10.1021/acsomega.4c05374
ACS Omega 2024, 9, 48185−48195

of the release properties, and the experiment was the normal *in vitro* release in a buffer solution. The difference in the observations between this work and Pagano and co-workers[5] can be attributed to the different formulation matrices. Although the results of this experiment indicated no apparent distinction between the permeation performance of the formulation containing neat FA and that containing nanohybrid, there are several advantages associated with nanohybrid over neat FA. Nanohybrid has multifunctional characteristics, such as sustained release of FA, protection of FA from degradation by solar exposure, and can act as a thickening agent. Thus, nanohybrids have great prospects of being used as FA carriers for topical delivery.

4. CONCLUSIONS

The intercalation of FA into two-dimensional Mg/Al LDH assisted in establishing an effective nanodelivery system for topical applications of FA. Analysis of the nanohybrid with appropriate characterization techniques ascertained the successful intercalation of FA into the interlayer galleries of Mg/Al LDH. The nanohybrids displayed a biphasic, pH-dependent, and continuous release of FA up to 6 h *in vitro*, evidence of remarkable controlled release attributes. The Franz diffusion cell experiments to assess skin permeation showed a linear correlation between the concentration of penetrated FA and time, signifying a gradual and effective release of FA from the nanohybrid in the formulation. Rheological experiments indicated that the presence of the nanohybrid in the topical formulation resulted in enhanced flow properties and may also improve the formulation stability. The DPPH antioxidant activity of the nanohybrid was not substantially different to that of free FA. The test compounds expressed no cytotoxicity in HaCaT cells, as the cell viability significantly increased in monolayer cultures after a 24-h incubation period. There was promising proof that nanohybrid is a promising multifunctional carrier and a transport system for the dermal and transdermal delivery of FA to address skin bioavailability and formulation efficacy.

AUTHOR INFORMATION

Corresponding Author

Suprakas Sinha Ray − *Centre for Nanostructured and Advanced Materials, DSI-CSIR Nanotechnology Innovation Centre, Council for Scientific and Industrial Research, Pretoria 0001, South Africa; Department of Chemical Sciences, University of Johannesburg, Johannesburg 2028, South Africa;* orcid.org/0000-0002-0007-2595; Email: rsuprakas@csir.co.za, ssinharay@uj.ac.za

Authors

Phumelele Kleyi − *Centre for Nanostructured and Advanced Materials, DSI-CSIR Nanotechnology Innovation Centre, Council for Scientific and Industrial Research, Pretoria 0001, South Africa*

Vusani Mandiwana − *Centre for Nanostructured and Advanced Materials, DSI-CSIR Nanotechnology Innovation Centre, Council for Scientific and Industrial Research, Pretoria 0001, South Africa*

Marinda de Beer − *Centre for Nanostructured and Advanced Materials, DSI-CSIR Nanotechnology Innovation Centre, Council for Scientific and Industrial Research, Pretoria 0001, South Africa*

Sreejarani Kesavan Pillai − *Centre for Nanostructured and Advanced Materials, DSI-CSIR Nanotechnology Innovation Centre, Council for Scientific and Industrial Research, Pretoria 0001, South Africa; Department of Chemical Sciences, University of Johannesburg, Johannesburg 2028, South Africa;* orcid.org/0000-0001-8015-2941

Complete contact information is available at: https://pubs.acs.org/10.1021/acsomega.4c05374

Notes

The authors declare no competing financial interest.

ACKNOWLEDGMENTS

We thank the Council for Scientific and Industrial Research (CSIR, Project No. C1E0080) and the Department of Science and Innovation (DSI, Project No. C6E0085), South Africa, for their financial support. Our gratitude is also extended to AMKA Products (Pty) Ltd., South Africa, for generously supplying the ingredients for the formulation preparation. We also acknowledge the support from the CeNAM characterization facility.

REFERENCES

(1) ULTRUS PROSPECTOR. https://www.ulprospector/en/na/PersonalCare/Deatail/473/318086/Folic-Acid/ (accessed March 25, 2024).

(2) L'Oreal Paris https://www.lorealparisusa.com/ingredient-library/folic-acid/ (accessed May 30, 2024).

(3) Debowska, R.; Rogiewicz, K.; Iwanenko, T.; Kruszewski, M.; Eris, I. Folic acid (Folacin) − New application of a cosmetic ingredient. *Kosmetische Med.* **2005**, *26*, 123−129.

(4) Rakuša, Ž. T.; Šenk, A.; Roškar, A. Content and stability of B complex vitamins in commercial cosmetic products. *J. Cosmet. Dermatol.* **2023**, *22*, 628−636.

(5) Pagano, C.; Perioli, L.; Latterini, L.; Nochetti, M.; Ceccarini, M. R.; Marani, M.; Ramella, D.; Ricci, M. Folic acid layered double hydroxides hybrids in skin formulations: technological, photochemical, and in vitro cytotoxicity on human keratinocytes and fibroblasts. *Appl. Clay Sci.* **2019**, *168*, 382−395.

(6) Choy, J.-H.; Jung, J.-S.; Oh, J.-M.; Park, M.; Jeong, J.; Kang, Y.-K.; Han, O.-J. Layered double hydroxide as an efficient drug reservoir for folate derivatives. *Biomaterials* **2004**, *25*, 3059−3064.

(7) Ozin, G. A. Nanochemistry synthesis in diminishing dimensions. *Adv. Mater.* **1992**, *4*, 612−649.

(8) Choy, J. H.; Park, N. G.; Hwang, S. J.; Kim, D. H.; Hur, N. H. New superconducting intercalation compounds: $(HgX_2)_{0.5}Bi_2Sr_2CaCu_2O_y$ (X = Br and I). *J. Am. Chem. Soc.* **1994**, *116*, 11564−11565.

(9) Choy, J. H.; Kwon, S. J.; Park, G. S. High-T_c superconductors in the 2D limit: $[(Py\text{-}C_nH_{2n+1})_2HgI_4]$-$Bi_2Sr_2Ca_{m-1}Cu_mO_y$ (m = 1 and 2). *Science* **1998**, *280*, 1589−1592.

(10) Kameliya, J.; Verma, A.; Dutta, P.; Arora, C.; Vyas, S.; Varma, R. S. Layered double hydroxide materials: A review on their preparation, characterization, and applications. *Inorganics* **2023**, *11*, 121.

(11) Soniya, V. P.; Bhindhu, P. S.; Rajalakshmi, K. Layered double hydroxides: Properties, synthesis, and its application in heavy metal remediation of soil. *Pharm. Innovations* **2023**, *12*, 1676−1680.

(12) Yazdani, P.; Mansouri, E.; Eyvazi, S.; Yousefi, V.; Kahroba, H.; Hejazi, S. M. M.; Mesbahi, A.; Tarhriz, V.; Tarhriz, V.; Abolghasemi, M. M. Layered double hydroxide nanoparticles as an appealing nanoparticle in gene/plasmid and drug delivery system in C2C12 myoblast cells. *Artif. Cells Nanomed. Biotechnol.* **2019**, *47*, 436−442.

(13) Senapati, S.; Sarkar, T.; Das, P.; Maiti, P. Layered double hydroxide nanoparticles for efficient gene delivery for cancer treatment. *Bioconjugate Chem.* **2019**, *30*, 2544−2554.

https://doi.org/10.1021/acsomega.4c05374
ACS Omega 2024, 9, 48185−48195

(14) Costard, L. S. S.; Kelly, D. C.; Power, R. N. N.; Hobbs, C.; Jaskaniec, S.; Nicolosi, V.; Cavanagh, B. L.; Curtin, C. M.; O'Brien, F. J. Layered double hydroxide as potent non-viral vector for nucleic acid delivery using gene-activated scaffolds for tissue engineering. *Pharmaceutics* **2020**, *12*, 1219.
(15) Yousefi, V.; Tarhriz, V.; Eyvazi, S.; Dilmaghani, A. Synthesis application of magnetic@layered double hydroxide as an anti-inflammatory drugs carrier. *J. Nanobiotechnol.* **2020**, *18*, 155.
(16) Peralta, M. F.; Mendieta, S. N.; Scolari, I. R.; Granero, G. E.; Crivello, M. E. Synthesis and release behaviour of layered double hydroxide-carbamazepine composites. *Sci. Rep.* **2021**, *11*, No. 20585.
(17) Zhang, Z.; Wells, C. J. R.; Liang, R.; Davies, G.-L.; Williams, G. R. Gadolinium doped layered double hydroxides for simultaneous drug delivery and magnetic resonance imaging. *J. Cluster Sci.* **2023**, *34*, 385−394.
(18) Molaei, M. J. Magnetic two-dimensional Ca-Al layered double hydroxide/Fe3O4@dextran nanocomposites as drug delivery systems. *J. Cryst. Growth* **2023**, *611*, No. 127186.
(19) Kleyi, P. E.; Mudaly, P.; Pillai, S. K.; de Beer, M. Zn/Al layered hydroxides nanostructure as effective controlled release vehicle of nicotinic acid for topical applications. *Appl. Clay Sci.* **2021**, *215*, 106304.
(20) Mavundza, E. J.; Tshikalange, T. E.; Lall, N.; Hussein, A. A.; Mudau, F. N.; Meyer, J. J. M. Antioxidant activity and cytotoxicity effect of flavonoids isolated from *anthrixia phylicoides*. *J. Med. Plants Res.* **2010**, *4*, 2584−2587.
(21) Pagano, C.; Tiralti, M. C.; Perioli, L. Nanostructured hybrids for the improvement of folic acid biopharmaceutical properties. *J. Pharm. Pharmacol* **2016**, *68*, 1384−1395.
(22) Qin, L.; Wang, W.; You, S.; Dong, J.; Zhou, Y.; Wang, J. *In vitro* antioxidant activity and in vivo antifatigue effect of layered double hydroxide nanoparticles as delivery vehicles for folic acid. *Int. J. Nanomed.* **2014**, *4*, 5701−5710.
(23) Cao, Y.; Fang, S.; Chen, K.; Qi, H.; Zhang, X.; Huang, C.; Wang, J.; Liu, J. Insight into the preparation of MgAl-layered double hydroxide (LDH) intercalated with nitrates and chloride adsorption ability study. *Appl. Sci.* **2022**, *12*, 4492.
(24) Roy, A. S.; Pillai, S. K.; Ray, S. S. A comparison of nitrate release from Zn/Al-, Mg/Al-, and Mg-Zn/Al layered double hydroxides and composite beads: Utilization of a slow-release filter. *ACS Omega* **2023**, *8*, 8427−8440.
(25) Qin, L.; Wang, S.; Zhang, R.; Zhu, R.; Sun, X.; Yao, S. Two different approaches to synthesizing Mg-Al-layered double hydroxides as folic acid carriers. *J. Phys. Chem. Solids* **2008**, *69*, 2779−2784.
(26) Xiao, R.; W Wang, W.; Pan, L.; Zhu, R.; Yu, Y.; Li, H.; Liu, H.; Wang, S.-L. A sustained folic acid release system based on ternary magnesium/zinc/aluminum layered double hydroxides. *J. Mater. Sci.* **2011**, *46*, 2635−2643.
(27) Magri, V. R.; Rocha, M. A.; de Matos, C. S.; Petersen, P. A. D.; Leroux, F.; Petrilli, H. M.; Constantino, V. R. I. Folic acid and folic acid salts: Thermal behavior and spectroscopic (IR, Raman, and solid state ^{13}C NMR) characterization. *Spectrochim. Acta, Part A* **2022**, *273*, No. 120981.
(28) Kim, T.-H.; Oh, J.-M. Dual nutraceutical hybrids of folic acid and calcium containing layered double hydroxides. *J. Solid State Chem.* **2016**, *233*, 125−132.
(29) Arízagal, G. G. C.; Jiminéz, C. S.; Saavedra, K. J. P.; Lamas, A. M. M.; Pérez, A. M. P. Folate-intercalated layered double hydroxide as a vehicle for cyclophosphamide, a non-ionic cancer drug. *Micro Nano Lett.* **2016**, *11*, 360−362.
(30) Cardinale, A. M.; Ciprioti, S. V.; Fortunato, M.; Catauro, M. Thermal behavior and antibacterial studies of a carbonate Mg-Al-based layered double hydroxide (LDH) for in vivo uses. *J. Therm. Anal. Calorim.* **2023**, *148*, 1523−1532.
(31) de Matos, C. S.; Rocha, M. A.; Taviot-Gueho, C. T.; Leroux, F.; Constantino, V. R. L. Layered Materials as Nanocarriers to Bioactive Molecules. In *Program Book*; Sociedade Brasileira de Pesquisa em Materiais: Rio de Janeiro, 2014.
(32) Mosangi, D.; Moyo, L.; Pillai, S. K.; Ray, S. S. Acetyl salicylic acid-ZnAl layered double hydroxide functional nanohybrid for skin care application. *RSC Adv.* **2016**, *6*, No. 105862.
(33) Li, L.; Warszawik, E.; van Rijn, P. pH-Triggered release and degradation mechanism of layered double hydroxides with high loading capacity. *Adv. Mater. Interfaces* **2023**, *10*, No. 2202396.
(34) Li, S.; Shen, Y.; Xiao, M.; Liu, D.; Fan, L. Synthesis and controlled release properties of *β*-naphthoxyacetic acid intercalated Mg-Al layered double hydroxides nanohybrids. *Arab. J. Chem.* **2019**, *12*, 2563−2571.
(35) Zhao, X.; Li, G.; Zhang, L.; Tao, X.; Guan, T.; Hong, M.; Tang, X. Preparation and evaluation of nicotinic acid sustained-release pellets combined with immediate release simvastatin. *Int. J. Pharm.* **2010**, *400*, 42−48.
(36) Gu, Z.; Thomas, A. C.; Xu, Z. P.; Campbell, J. H.; Lu, G. Q. *In vitro* sustained release of LMWH from MgAl-layered double hydroxidenanohybrids. *Chem. Mater.* **2008**, *20*, 3715−3722.
(37) Ambrogi, V.; Guiseppe, F.; Grandolini, G.; Perioli, L.; Titalti, M. C. Intercalation compounds of hydrotalcite-like anionic clays with anti-inflammatory agents. II. Uptake of diclofenac for a controlled release formulation. *AAPS PharmSciTech* **2002**, *3*, No. 26, DOI: 10.1208/pt030326.
(38) Poe, M. Acid dissociation constants of folic acid, dihydrofolic acid, and methotrexate. *J. Biol. Chem.* **1977**, *252*, 3724−3728.
(39) Lin, Y.; Huang, Z.; Zhuo, R.; Fang, J. Combination of calcipotrioland methotrexate in nanostructured lipid carriers for topical delivery. *Int. J. Nanomed.* **2010**, *5*, 117−128.
(40) Liu, J.; Zhao, Q.; Zhang, X. Structure and slow release properties of chlorpyrifos/graphene oxide-ZnAl layered double hydroxide composite. *Appl. Clay Sci.* **2017**, *145*, 44−52.
(41) Jin, L.; Liu, Q.; Sun, Z.; Ni, X.; Wei, M. Preparation of 5-fluorouracil/cyclodextrin complex intercalated in layered double hydroxide and the controlled drug release properties. *Ind. Eng. Chem. Res.* **2010**, *49*, 11176−11181.
(42) Conastatino, U.; Casciola, M.; Massinelli, L.; Nocchetti, M.; Vivani, R. Intercalation and grafting of hydrogen phosphates and phosphonates into synthetic hydrotalcitesand a.c.-conductivity of compounds thereby obtained. *Solid State Ionics* **1997**, *97*, 203−212.
(43) Lonkar, S. P.; Kutlu, B.; Leuteritz, A.; Heinrich, G. Nanohybrids of phenolic antioxidant intercalated into Mg/Al-layered double hydroxide clay. *Appl. Clay Sci.* **2013**, *71*, 8−14.
(44) Ansy, K. M.; Lee, J.-H.; Piao, H.; Choi, G.; Choy, J.-H. Stabilization of antioxidant gallate in layered double hydroxide by exfoliation and reassembling reaction. *Solid State Sci.* **2018**, *80*, 67−71.
(45) Szerlauth, A.; Muráth, S.; Szilagyi, I. Layered double hydroxide-based antioxidant dispersions with high colloidal and functional stability. *Soft Matter* **2020**, *16*, 10518−10527.
(46) Cianciulli, A.; Salvatore, R.; Porro, C.; Trotta, T.; Panaro, M. A. Folic acid is able to polarize the inflammatory response in LPS activated microglia by regulating multiple signalling pathways. *Mediat. Inflamm.* **2016**, *2016*, 5240127.
(47) Samblas, M.; Martínez, A.; Milagro, F. Folic acid improves the inflammatory response in LPS-activated THP-1 macrophages. *Mediat. Inflamm.* **2018**, *2018*, No. 1312626.
(48) Metzger, T. G. *Applied Rheology with Joe Flow on Rheology Road*; Anton-Paar GmbH: Germany, 2021; p 89.
(49) Park, E.-K.; Song, K.-W. Rheological evaluation of petroleum jelly as a base material in ointment and cream formulations: Steady shear flow behavior. *Arch. Pharm. Res.* **2010**, *33*, 141−150.
(50) Perioli, L.; Pagano, C.; Nochetti, M.; Latterini, L. Development of smart semi-solid formulations to enhance retinoic acid topical application. *J. Pharm. Sci.* **2015**, *104*, 3904−3912 2015.
(51) Pagano, C.; Calarco, P.; Ceccarini, M. R.; Beccari, T.; Ricci, M.; Perioli, L. Development and characterization of new topical hydrogels based on alpha-lipoic acid − hydrotalcite hybrids. *Cosmetics* **2019**, *6*, 35.
(52) Brummer, R. *Rheology Essentials of Cosmetic and Food Emulsions*; Springer-Verlag: Berlin, 2006.

https://doi.org/10.1021/acsomega.4c05374
ACS Omega 2024, 9, 48185−48195

(53) Carli, B. Diploma in Personal Care Formulations, Module 2, 4th ed. ISBN 978-0-9874089-3-8.
(54) Garti, N. Hydrocolloids as emulsifying agents for oil-in-water emulsions. *J. Dispersion Sci. Technol.* **1999**, *20*, 327−355.
(55) Thorgeirsdóttir, T. s.; Thormar, H.; Kristmundsdóttir, T. Viscoelastic properties of a virucidal cream containing the monoglyceride monocaprin: effects of formulation variables: a technical note. *AAPS PharmSciTech* **2006**, *7*, E95−E98.
(56) Mosangi, D.; Pillai, S. K.; Moyo, L.; Ray, S. S. Rheological characteristics of petroleum jelly formulations containing organically modified layered double hydroxides. *J. Appl. Chem. Sci. Int.* **2018**, *9*, 104−114.
(57) Dabbaghi, M.; Namjoshi, S.; Panchal, B.; Grice, J. E.; Prakash, S.; Roberts, M. S.; Mohammed, Y. Viscoelastic and Deformation Characteristics of Structurally Different Commercial Topical Systems. *Pharmaceutics* **2021**, *13*, 1351.
(58) Perioli, L.; Mutascio, P.; Pagano, C. Influence of the nanocomposite MgAl-HTlc on gastric absorption of drugs: *In vitro* and *ex vivo* studies. *Pharm. Res.* **2013**, *30*, 156−166.
(59) Khan, A. I.; Lei, L.; Norquist, A. J.; O'Hare, D. Intercalation and controlled release of pharmaceutically active compounds from a layered double hydroxide. *Chem. Commun.* **2001**, 2342−2343.
(60) Mallakpour, S.; Hatami, M. Highly capable and cost-effective chitosan nanocomposite films containing folic-acid-functionalized layered double hydroxide and their *in vitro* bioactive performance. *Mater. Chem. Phys.* **2020**, *250*, No. 123044.

https://doi.org/10.1021/acsomega.4c05374
ACS Omega 2024, 9, 48185−48195